Miniemulsion Polymerization Using Oil-Soluble Initiators

Juan A. Alduncin, Jacqueline Forcada, and José M. Asua*

Grupo de Ingeniería Química, Departamento de Química Aplicada, Facultad de Ciencias Químicas, Universidad del País Vasco, Apdo 1072, 20080 San Sebastián, Spain

Received April 15, 1993; Revised Manuscript Received December 12, 1993®

ABSTRACT: The ability of a series of initiators with different water solubilities (lauroyl peroxide, benzoyl peroxide, and azobis(isobutyronitrile)) in stabilizing monomer droplets against degradation by molecular diffusion was investigated in the batch miniemulsion polymerization of styrene. Comparison of the evolution of the particle size distributions obtained in these experiments with those of a series of miniemulsion polymerizations where the stability of the monomer droplets was ensured by using hexadecane in addition to the oil-soluble initiators showed that only lauroyl peroxide was water-insoluble enough to stabilize the monomer droplets against degradation by molecular diffusion. The results were analyzed by a mathematical model.

Introduction

The main characteristic of miniemulsion polymerization is that particle nucleation occurs in submicron monomer droplets.[1,2] These submicron monomer droplets are produced from a mixture of monomer, water, emulsifier, and a water-insoluble compound by using a pressure homogenizer, colloid mill, or ultrasound device. This water-insoluble compound is a fatty alcohol or a long-chain alkane. It should be noted that both linear and branched molecules can be used provided that they have the same water solubility. The emulsifier provides stability against coagulation. The role of the water-insoluble compound, mainly in the case of long-chain alkanes, is to prevent degradation of the miniemulsion due to the Ostwald ripening effect, namely, the diffusion of monomer from the small to large droplets to minimize the interfacial free energy of the system. The water-insoluble compound remains in the polymer particles after polymerization and may have a deleterious effect on the properties of the polymer. This effect might be reduced to some extent if the water-insoluble compound is covalently bonded to the polymer chain. This might, in principle, be achieved by using water-insoluble chain transfer agents or initiators. Several authors have study the effect of highly water-insoluble chain transfer agents such as *n*-dodecyl mercaptan (water solubility 3×10^{-5} mol/L) on the kinetics of conventional emulsion polymerization systems.[3-6] However, none of them have tried to carry out a miniemulsion polymerization. In the patent literature, Ugelstad[7] disclosed a process for the preparation of polymer latexes that involves the emulsification of an initiator or initiator mixture in the presence of an emulsifier in water in a first step and adding monomer and polymerizing in a second step. To avoid the degradation of the monomer droplets by molecular diffusion, the initiator or initiator mixture should have a water solubility lower than 10^{-4} g/L. In addition, their melting point has to be low enough to allow emulsification at a temperature below the decomposition temperature of the initiator(s).

In the present work, the ability of a series of initiators with different water solubilities in stabilizing monomer droplets against degradation by molecular diffusion was investigated in the batch miniemulsion polymerization of styrene.

Table 1. Values of the Parameters Used in the Calculations

	LPO	BPO	AIBN
water solubility (g/100 g of H_2O)	2×10^{-9} [a]	3×10^{-4} [a]	0.04[d]
k_I (s^{-1})	1×10^{-4} [b]	1.83×10^{-5} [c]	9.25×10^{-5} [c]
f	0.6	0.6	0.6

$k_p = 4.13 \times 10^5$ cm^3 mol^{-1} s^{-1} [e] $k_t = 1.11 \times 10^4$ cm^3 mol^{-1} s^{-1} [f]
$D_w = D_d = 10^{-6}$ cm^2/s $F = 10^{-5}$

[a] Reference 11. [b] Reference 8. [c] Reference 9. [d] Reference 10. [e] Reference 17. [f] Reference 18.

Table 2. Recipes Used in the Polymerizations (T = 75 °C)

	miniemulsion polymerization	"classical" miniemulsion polymerization
styrene (g)	144.6	144.6
sodium lauryl sulfate (g)	1.237	1.237
initiator (g)	3.624	3.624
hexadecane (g)		3.289
DDI water (g)	455.2	455.2

Experimental Section

Styrene was distilled under reduced pressure and stored at −18 °C until used. Distilled and deionized water (DDI) was used throughout the work. The other materials were used as received. Azobis(isobutyronitrile) (AIBN), benzoyl peroxide (BPO), and lauroyl peroxide (LPO) were used as initiators. The water solubilities of these initiators are given in Table 1.

Miniemulsions were made by using the recipe given in Table 2 by mixing a solution of emulsifier in water with another of initiator in monomer. Then the system was subjected to sonication (Branson Sonifier 450) at room temperature under agitation provided by a magnetic bar stirrer. The conditions for the sonication were as follows: output control, 8; duty cycle, 80%; sonication time, 2 min. After sonication, droplet size measurements were carried out by dynamic light scattering (DLS) using a Malvern 4700 apparatus. To make these measurements, a sample of miniemulsion inhibited with hydroquinone was diluted to the appropriate level in water saturated with styrene. The shelf life stability of the miniemulsion was studied by measuring the time evolution of the droplet size. A sample of each miniemulsion inhibited with hydroquinone was placed in a capped glass flask and kept under gentle agitation provided by a magnetic stirrer for at least 2 h. Periodically, samples were withdrawn from the flask and the droplet size was measured as described above.

To carry out the polymerizations, the miniemulsion was charged into a 1-L glass unbaffled jacketed reactor preheated to 75 °C and equipped with a reflux condenser, stainless steel stirrer, nitrogen inlet, and sampling device. All the polymerizations were carried out at 75 °C using a stirrer speed of 200 rpm. Samples were withdrawn during the process, and the polymerization was

* To whom correspondence should be addressed.
® Abstract published in *Advance ACS Abstracts*, March 15, 1994.

0024-9297/94/2227-2256$04.50/0

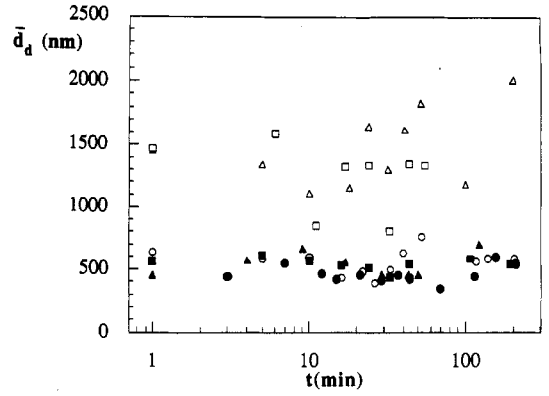

Figure 1. Time evolution of the droplet diameter for the different miniemulsions. Legend: (○) LPO; (●) LPO + HD; (△) BPO; (▲) BPO + HD; (□) AIBN; (■) AIBN + HD.

quenched with hydroquinone. The conversion was determined by gravimetry, and the particle size was measured by transmission electron microscopy (TEM). Particle size distribution (PSD) was determined by means of a graphics tablet (Summasketch Plus).

For the sake of comparison, a series of miniemulsion polymerizations were carried out using the same procedure as in the previous series but including hexadecane (HD) in addition to the oil-soluble initiator (Table 2). These miniemulsion polymerizations will be denoted as "classical" miniemulsion polymerizations.

Results and Discussion

Shelf Life Stability. To determine the extent of the monomer droplet degradation in a scale of time similar to that of the polymerization, the monomer droplet size was measured by DLS following the procedure described above. These sizes will be later compared with those of the latexes resulting from polymerizing these miniemulsions measured by TEM. However, the Malvern 4700 gives the z-average diameter, which is different from the volume-average diameter measured by TEM. Zamora[12] carried out a comparison between the z-average diameters measured by the Malvern 4700 and the volume-average diameters measured by TEM for polydisperse latexes in the range 100–400 nm, obtaining the following relationship:

$$d_{p,TEM} = 0.8 d_{p_z} \tag{1}$$

Although the difference between the two diameters might increase with the particle diameter, in the present paper it has been assumed that, as a first approximation, eq 1 holds for the whole range of droplet sizes. Figure 1 presents the time evolution of the volume-average-equivalent droplet diameters calculated by eq 1 from the z-averages measured by DLS. Although the data are affected by significant experimental noise, it can be seen that the miniemulsions containing LPO had droplet sizes similar to those of the classical miniemulsion polymerizations. The particle size of these miniemulsions remained roughly constant for more than 2 h after the sonication; i.e., they were stable. Figure 1 shows that the average size of the miniemulsions containing BPO and AIBN was very large. These results suggest that these miniemulsions suffered a quick partial degradation after sonication.

Miniemulsion Polymerizations. Figure 2 presents the evolution of the PSD during the miniemulsion polymerization initiated by LPO. It can be seen that a broad PSD was obtained. Measured particle sizes ranged from 20 to over 3000 nm. A log–log plot was used because, although the number of large polymer particles is small,

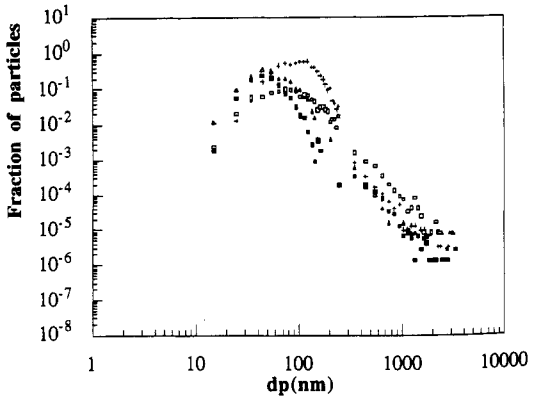

Figure 2. Evolution of the particle size distribution in the miniemulsion polymerization initiated by LPO. Legend: (■) x = 0.26; (△) x = 0.43; (+) x = 0.67; (■) x = 0.92.

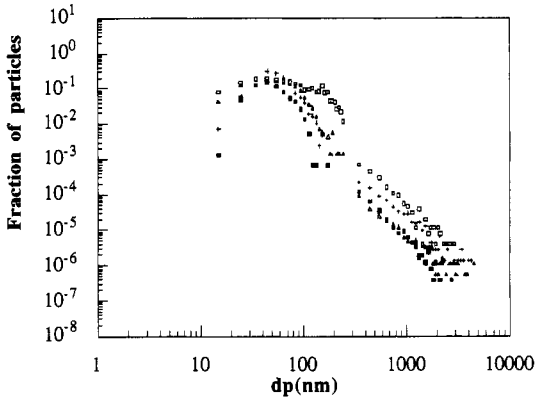

Figure 3. Evolution of the particle size distribution in the miniemulsion polymerization initiated by LPO and costabilized by HD. Legend: (■) x = 0.07; (△) x = 0.26; (+) x = 0.52; (□) x = 0.88.

they substantially contributed to the total volume of polymer. The apparent discontinuity in the region of 250 nm is an artifact due to the fact that below 250 nm the polymer particles were divided into 10-nm size classes, and above 250 nm the size of each class was 100 nm. This was adequately accounted for in the normalization. In addition, the different PSDs were normalized to each other, taking into account their corresponding conversions as follows:

$$\frac{1}{x}\sum_i h_i v_i = k_1 \tag{2}$$

where x is the conversion, h_i is the fraction of particles, v_i is the average volume of the class, and k_1 is an arbitrary constant equal for all PSDs. This normalization allows the direct comparison between the different particle size distributions.

Figure 2 shows that large particles were formed from the beginning of the process (conversion = 0.26) and that the number of large polymer particles increased during polymerization. In addition, the presence of tiny polymer particles during the whole process suggests that continuous nucleation occurred.

Figure 3 presents the PSD evolution in the miniemulsion polymerization initiated by LPO and costabilized with hexadecane, namely, a classical miniemulsion polymerization. It can be seen that the PSD was very similar to that obtained with LPO alone. This suggests that the mechanisms controlling the nucleation process are not significantly affected by the addition of HD. A closer comparison shows that the number of large particles was

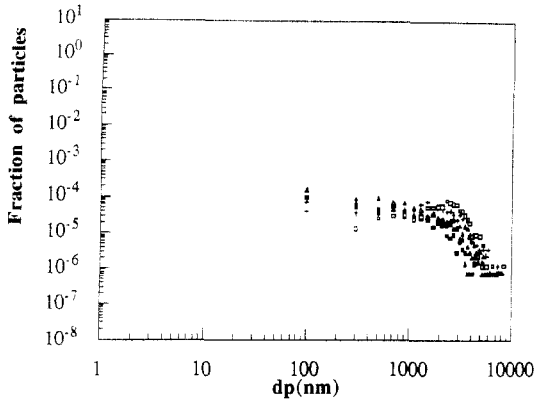

Figure 4. Evolution of the particle size distribution in the miniemulsion polymerization initiated by BPO. Legend: (■) x = 0.12; (△) x = 0.20; (▲) x = 0.38; (+) x = 0.63; (□) x = 0.88.

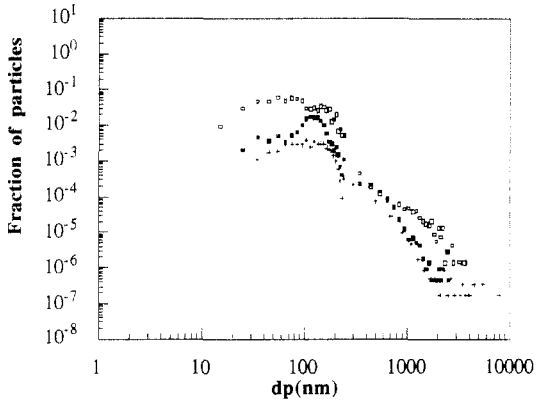

Figure 5. Evolution of the particle size distribution in the miniemulsion polymerization initiated by BPO and costabilized by HD. Legend: (■) x = 0.12; (+) x = 0.29; (□) x = 0.81.

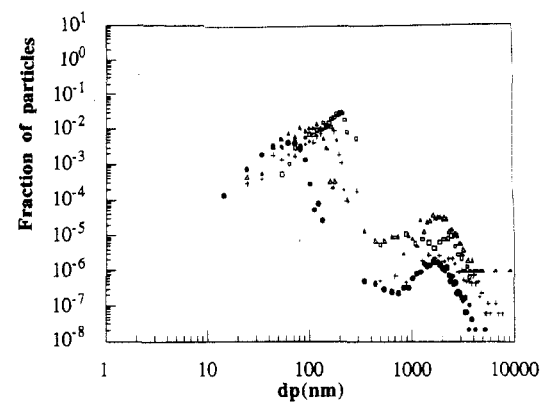

Figure 6. Evolution of the particle size distribution in the miniemulsion polymerization initiated by AIBN. Legend: (●) x = 0.09; (△) x = 0.28; (+) x = 0.61; (□) x = 0.88.

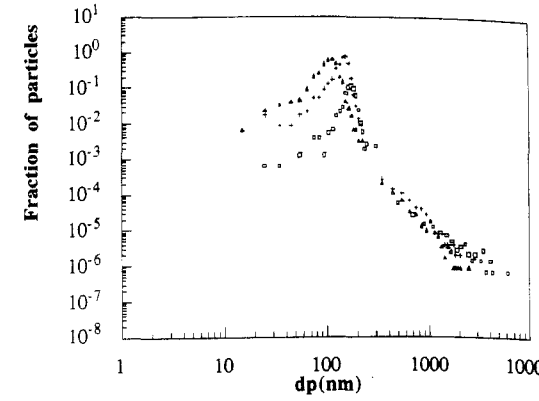

Figure 7. Evolution of the particle size distribution in the miniemulsion polymerization initiated by AIBN and costabilized by HD. Legend: (△) x = 0.34; (+) x = 0.64; (□) x = 0.95.

slightly lower for the miniemulsion polymerization costabilized with HD.

Figure 4 presents the evolution of the PSD in the miniemulsion polymerizations initiated by BPO. The same scale as in the previous figures was used to make easier the comparison between the results obtained in the different processes. Figure 4 shows that the latex obtained with BPO contained mainly large polymer particles, and, hence, a lower number of polymer particles was obtained.

Figure 5 presents the evolution of the PSD in the miniemulsion polymerization initiated by BPO and costabilized with HD, i.e., a classical miniemulsion polymerization. It can be seen that a broad PSD similar to those obtained with LPO was obtained. Comparison with Figure 4 shows that HD strongly influenced the nucleation process. In addition, the presence of small particles in the high-conversion samples suggests that continuous nucleation occurred.

Figure 6 presents the evolution of the PSD in the miniemulsion polymerization initiated by AIBN. It can be seen that a bimodal particle size distribution was obtained. The size of the largest mode is 3 orders of magnitude (in volume) over that of the small mode. This excludes the possibility that the large particles were formed by coagulation of the small ones, because if this were the case, modes at intermediate volumes should appear in the PSD.

Figure 7 presents the evolution of the PSD in a classical miniemulsion polymerization (i.e., costabilized with HD) initiated by AIBN. These PSDs were similar to those obtained in the other classical miniemulsion polymerizations (Figures 3 and 5). However, in the AIBN-initiated process, the peak of small polymer particles was narrower than in the other processes and the number of small particles decreased at the end of the polymerization.

The results presented in Figures 2–7 can be summarized as follows:

(i) The particle size distributions obtained in the classical miniemulsion polymerizations, i.e., including hexadecane in the recipe, were not significantly affected by the initiator used even though they have very different water solubilities and decomposition rates. Nevertheless, closer examination of these PSDs reveals that the number of large polymer particles was greater in the case of the BPO-initiated process than for the other two processes. In addition, continuous generation of small polymer particles was observed during the miniemulsion polymerizations initiated by LPO and BPO while this phenomenon was not evident in the miniemulsion polymerization initiated by AIBN, although it cannot be discarded.

(ii) The PSD obtained in the miniemulsion polymerization initiated by LPO with no HD in the recipe was similar to that obtained in the presence of HD, although the number of large polymer particles was slightly higher for the former case.

(iii) The latex obtained in the miniemulsion polymerization initiated by BPO without HD in the recipe contained mainly large polymer particles.

(iv) A bimodal PSD was obtained when AIBN was used alone, the size of the large mode being 3 orders of magnitude (in volume) greater than the small one.

To account for these results, the mechanisms illustrated in Figure 8 are proposed. At the beginning of the process, there is a miniemulsion of monomer, initiator, hexadecane if present, and emulsifier in water. Let us consider first the case of classical miniemulsion polymerizations, i.e.,

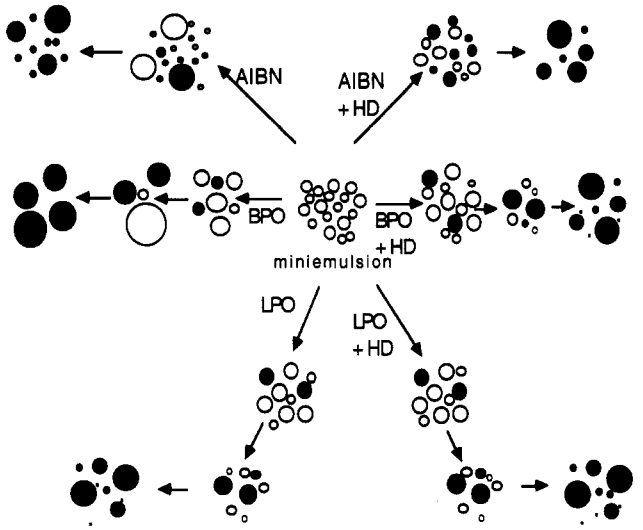

Figure 8. Scheme of the mechanisms proposed to describe the process occurring during the miniemulsion polymerizations. Legend: (○) monomer droplets; (●) polymer particles.

including HD in the recipe. Figure 1 shows that these miniemulsions were stable in the time scale of the polymerization. Upon heating, the initiator decomposes, giving free radicals that start polymerization in some monomer droplets, namely, nucleating polymer particles. Intuitively, one would expect that the probability of nucleation of monomer droplets be dependent upon the droplet size. The probability of nucleation is closely related to the probability of formation of a long enough polymer chain in the monomer droplet. A polymer chain will be formed whenever a single radical appears in the monomer droplet. "Single radicals" refers to radicals that appear in the monomer droplets one at a time as oppossed to pair generation in which, due to initiator decomposition, two radicals appear in the monomer droplet at the same time. Single radicals can be formed by desorption of one of the radicals formed by initiator decomposition and by entry of a radical from the aqueous phase. In the aqueous phase, radicals appear by decomposition of the fraction of oil-soluble initiator dissolved in the water and by desorption of radicals from the oil phase. A monomer droplet will also be nucleated if the pair of radicals formed from the initiator in the monomer droplet does not suffer instantaneous bimolecular termination. The mechanisms involved in the formation and transfer of radicals between phases have been modeled by Asua et al.[13] According to these authors, the net rate of formation of single radicals inside a monomer droplet of volume v_d is

$$R_I(v_d) = 2fk_I N_A[I]v_d(1-f_w)(f_d - f_d^2)\ \frac{\text{radicals}}{\text{particle second}} \quad (3)$$

where f is the initiator efficiency, k_I is the rate constant for initiator decomposition, N_A is Avogadro's number, [I] is the initiator concentration in the monomer droplets, f_w is the fraction of the initiator dissolved in the aqueous phase, and f_d is the fraction of initiator radicals that desorb given by the competition between the desorption rate and the rates of termination and propagation:

$$f_d = \frac{k_{0I}}{k_{0I} + k_p[M] + k_t/(v_d N_A)} \quad (4)$$

where k_{0I} is the rate of exit of an initiator radical, k_p is the propagation rate constant, and k_t is the termination rate constant. According to Nomura,[14] k_{0I} is given by

$$k_{0I} = \frac{12D_w/(m_I d_d^2)}{1 + 2D_w/(m_I D_d)} \quad (5)$$

where D_w and D_d are the diffusion coefficients of the radicals in the aqueous phase and monomer droplets, respectively, m_I is the partition coefficient of the initiator radicals between monomer droplets and aqueous phase, and d_d is the monomer droplet diameter.

Single radicals can also appear by radical entry. The rate of radical absorption is expressed as

$$R_a(v_d) = k_a[R]_w\ \frac{\text{radicals}}{\text{particle second}} \quad (6)$$

where $[R]_w$ is the concentration of radicals in the aqueous phase and k_a is the absorption rate coefficient. If the absorption of radicals occurs through a diffusion process, k_a is given by[15]

$$k_a = 2\pi D_w d_d N_A F \quad (7)$$

where F is the radical capture efficiency.

Monomer droplets can also be nucleated if the pair of radicals formed from the initiator in the monomer droplet propagates significantly before bimolecular termination occurs. In this work, the length of the polymer chain to consider that a monomer droplet is nucleated was assumed to be 200. With this assumption, the rate of nucleation of monomer droplets by growth of the pair of initiator radicals is as follows:

$$R_p(v_d) = [fk_I N_A[I]v_d(1-f_w)(1-f_d)^2]P^{100}\ \frac{\text{pairs of radicals}}{\text{particle second}} \quad (8)$$

where the term between brackets is the rate of formation of pairs of radicals in the monomer droplet[13] and P is the probability of propagation given by the competition between the propagation rate and the rate of termination:

$$P = \frac{k_p[M]}{k_p[M] + k_t/(N_A v_d)} \quad (9)$$

Equation 8 includes P to the 100th power because termination occurs by combination.

The overall rate of nucleation of monomer droplets of volume v_d is as follows:

$$R_{nuc}(v_d) = R_I(v_d) + R_a(v_d) + R_p(v_d)\ \frac{\text{droplets}}{\text{droplet second}} \quad (10)$$

The rigorous calculation of $R_{nuc}(v_d)$ is rather complex because the calculation of $[R]_w$ requires the determination of the free-radical distribution in polydisperse systems using oil-soluble initiator. Nevertheless, useful information about the relative dependence of the nucleation rates on the droplet size can be obtained by considering monodisperse systems of varying droplet sizes. Figure 9 presents for the three initiators used the effect of the droplet size on the nucleation rate relative to the nucleation rate of 100-nm-diameter monomer droplets initiated by LPO. The parameters given in Table 1 were used in these calculations. It can be seen that the probability of nucleation increases sharply with the droplet size. This means that large monomer droplets are expected to be more easily nucleated than small ones. This explains why large polymer particles appeared soon in the polymerization. As polymerization proceeds, monomer diffuses from the monomer droplets to the growing polymer

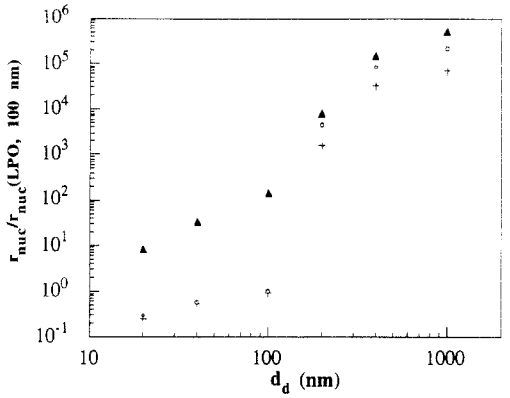

Figure 9. Effect of the droplet size on the nulceation rate relative to the nucleation rate of 100-nm-diameter monomer droplets initiated by LPO. Legend: (○) LPO; (+) BPO; (▲) AIBN.

particles. Consequently, the size of the monomer droplets decreased. Figure 9 also shows that the probability of nucleation of droplets is larger for AIBN than for LPO which is larger than that for BPO. It is expected that the larger the nucleation rate is, the lower the number of large particles. In agreement with the expected results, Figures 3, 5, and 7 show that, for similar conversions, the number of large polymer particles is lower for AIBN that for LPO which is lower than for BPO.

In miniemulsion polymerization, droplet–droplet coagulation and droplet–particle coagulation may also decrease the number of monomer droplets. Because of both the experimental difficulties in measuring the droplet size distributions of the miniemulsions by DLS and the limitations of the software of the Malvern apparatus, the available measurements of these distributions were not reliable enough to assess through comparison with the PSDs of the latexes if coagulation occurred during the process. Nevertheless, coagulation would depend on the emulsifier used and the agitation conditions. All reactions were carried out using the same amount of emulsifier and agitation conditions; therefore the differences in PSD cannot be attributed to a coagulation process.

The Ostwald ripening effect can be counteracted if the monomer droplets contain a compound that does not diffuse through the aqueous phase in the characteristic time of the polymerization. The lower the water solubility of this compound is, the lower its diffusion rate through the aqueous phase and the less important the Ostwald ripening effect. Hexadecane is substantially insoluble in water; therefore when it was included in the recipe, the Ostwald ripening effect was minimized (Figure 1) and monomer droplets remained in the reactor until the last stages of the polymerization.

Figures 3 and 5 show that continuous nucleation of monomer droplets occurred during the classical miniemulsion polymerizations initiated by LPO and BPO. In addition, the number of small polymer particles increased during the polymerization. On the other hand, in the classical miniemulsion polymerization initiated by AIBN, there were small particles during the whole process but their number decreased in the last stages of the process. The continuous nucleation can occur by nucleation of monomer droplets, micellar nucleation, or homogeneous nucleation. Due to the small size of the miniemulsion droplets, the number of micelles is low as compared with a conventional emulsion polymerization. In addition, micellear and homogeneous nucleations involve water-soluble radicals, and hence they will not likely occur in the classical miniemulsion polymerization initiated by oil-soluble initiators. Therefore, nucleation of monomer droplets seems to be the more likely mechanism for these initiators.

Table 3. Effect of the Particle Size on the Average Number of Radicals per Particle

particle diam (nm)	$\bar{n}$		
	LPO	BPO	AIBN
20	0.00078	0.00063	0.02
40	0.0053	0.0045	0.18
100	0.053	0.041	0.48
200	0.43	0.24	0.74
400	3.6	1.94	5.3
1000	17.5	9.62	26.2

The differences between the initiators can be explained by taking into account that, as Figure 9 shows, the probability of nucleation is much larger for AIBN than in the cases of LPO and BPO. Additional explanation can be found by considering the results presented in Table 3. This table presents the effect of the particle size on the average number of radicals per particle calculated by the approach proposed by Asua et al.[13] with the parameters given in Table 1. It can be seen that $\bar{n}$ is much higher for AIBN than for LPO and BPO and that the smaller the polymer particle is, the larger the difference. This means that in the polymerization initiated by AIBN the small polymer particles can grow during the process whereas in the polymerizations initiated by LPO and BPO the polymerization rate is extremely slow and hence the small polymer particles will remain almost unchanged during the process.

The PSD obtained in the miniemulsion polymerization initiated by LPO without HD in the recipe is similar to that obtained in the presence of HD because LPO is almost water-insoluble and therefore it is able to counteract the Ostwald ripening effect (Figure 1). The fact that the number of large polymer particles is lower when HD was included in the recipe may be due to the contribution of HD to the stability of the monomer droplets against the Ostwald ripening effect.

When BPO was used alone, only large particles were obtained; this indicates that, as shown in Figure 1, BPO is not water-insoluble enough to avoid monomer droplet degradation by the Ostwald ripening effect. Therefore, from the beginning of the process, monomer diffuses from small to large droplets, and soon the system includes only growing polymer particles and large monomer droplets. These large monomer droplets act both as monomer reservoirs and as nucleation loci.

Monomer droplet degradation by the Ostwald ripening effect is even more acute in the polymerizations carried out with AIBN alone. The bimodal PSD may result from the combined effect of a large nucleation rate and a rapid monomer droplet degradation (see Figure 1), the small particles being the result of nucleation in monomer droplets before they disappear by monomer diffusion and the large ones coming from nucleation in the growing large monomer droplets.

Conclusions

In the foregoing, batch miniemulsion polymerizations of styrene were carried out using oil-soluble initiators of different water solubilities as a means of avoiding the monomer droplet degradation by the Ostwald ripening effect. For the sake of comparison, a series of miniemulsion polymerizations were carried out including hexadecane in the recipe in addition to the oil-soluble initiators. It was found that the miniemulsion polymerizations carried out with LPO led to a broad particle size distribution similar to that of the miniemulsion polymerization costabilized

with HD. On the other hand, BPO and AIBN are not water-insoluble enough to avoid the Ostwald ripening effect and extensive monomer droplet degradation occurred. In addition, it was found that the PSD obtained in the presence of HD was not significantly affected by the initiator used even though they have very different water solubilities and decomposition rates.

Acknowledgment. Financial support by the Excma. Diputación Foral de Gipuzkoa is gratefully appreciated.

Nomenclature

d_d monomer droplet diameter (nm)
$d_{p,TEM}$ particle diameter measured by transmission electron microscopy (nm)
d_{pz} particle diameter measured by dynamic light scattering (nm)
D_d diffusion coefficient of the radicals in the monomer droplets (cm^2/s)
D_w diffusion coefficient of the radicals in the aqueous phase (cm^2/s)
f initiator efficiency
F radical capture efficiency
f_d fraction of initiator radicals that desorb from the monomer droplets
f_w fraction of the initiator dissolved in the aqueous phase
h_i fraction of particles
[I] initiator concentration (mol/cm^3)
k_a absorption rate coefficient ($cm^3\ mol^{-1}\ s^{-1}$)
k_I rate constant for initiator decomposition (s^{-1})
k_{0I} rate of exit of an initiator radical (s^{-1})
k_p propagation rate constant ($cm^3\ mol^{-1}\ s^{-1}$)
k_t termination rate constant ($cm^3\ mol^{-1}\ s^{-1}$)
[M] monomer concentration in the monomer droplets (mol/cm^3)
m_I partition coefficient of the initiator radicals between monomer droplets and the aqueous phase
$\bar{n}$ average number of radicals per particle
N_A Avogadro's number
P probability of propagation
R_a rate of radical absorption
R_I rate of formation of single radicals inside a monomer droplet
R_{nuc} overall rate of nucleation of monomer droplets
R_p rate of nucleation of monomer droplets by growth of a pair of initiator radicals
$[R]_w$ concentration of radicals in the aqueous phase (mol/cm^3)
v_d monomer droplet volume (cm^3)
v_i average volume of the particles of the class i
x conversion

References and Notes

(1) Ugelstad, J.; El-Aasser, M. S.; Vanderhoff, J. W. *J. Polym. Sci., Polym. Lett. Ed.* **1973**, *11*, 503.
(2) Delgado, J.; El-Aasser, M. S. *Makromol. Chem., Macromol. Symp.* **1990**, *31*, 63.
(3) Kolthoff, I. M.; Dale, W. J. *J. Am. Chem. Soc.* **1945**, *67*, 1672.
(4) Nomura, M.; Minamino, Y.; Fujita, K. *J. Polym. Sci. Polym. Chem. Ed.* **1982**, *20*, 1261.
(5) Lee, H. C.; Poehlein, G. W. *Polym. Process. Eng.* **1987**, *5*(1), 37.
(6) Song, Z.; Poehlein, G. W. *Polym.-Plast. Technol. Eng.* **1990**, *29*(4), 377.
(7) Ugelstad, J. European Patent 0010986 A1, 1980.
(8) Breintenbach, J. W.; Schindler, A. *Monatsh. Chem.* **1952**, *83*, 724.
(9) Redington, L. E. *J. Polym. Sci.* **1948**, *3*, 503.
(10) Kirk, R. E.; Othmer, D. F. In *Encyclopedia of Chemical Technology*; Wiley-Interscience: New York, 1978; Vol. 15, p 902.
(11) Yalkowsky, S. H.; Banerjee, S. In *Aqueous Solubility. Methods of Estimation for Organic Compounds*; Marcel Dekker Inc.: New York, 1992.
(12) Zamora, A. Ph.D. Dissertation, Universidad del País Vasco, San Sebastián, 1991.
(13) Asua, J. M.; Rodríguez, V. S.; Sudol, E. D.; El-Aasser, M. S. *J. Polym. Sci., Part A: Chem. Ed.* **1989**, *27*, 3569.
(14) Nomura, M. In *Emulsion Polymerization*; Piirma, I., Ed.; Academic Press: New York, 1982.
(15) Ugelstad, J.; Hansen, F. K. *Rubber Chem. Technol.* **1976**, *49*(3), 536.
(16) Asua, J. M.; Rodríguez, V. S.; Silebi, C. A.; El-Aasser, M. S. *Makromol. Chem., Macromol. Symp.* **1990**, *35/36*, 59.
(17) Cheng, S. A.; Jeng, W. F. *Chem. Eng. Sci.* **1978**, *33*, 735.
(18) Hui, A.; Hamielec, A. E. *J. Appl. Polym. Sci.* **1972**, *16*, 749.